

1 **Impaired adipocyte SLC7A10 promotes lipid storage**  
2 **in association with insulin resistance and altered BCAA metabolism**

3  
4 Regine Å. Jersin<sup>1,2\*</sup>, Divya Sri Priyanka Tallapragada<sup>1,2\*</sup>, Linn Skartveit<sup>1,2</sup>, Mona S. Bjune<sup>1,2</sup>,  
5 Maheswary Muniandy<sup>3</sup>, Sindre Lee-Ødegård<sup>4</sup>, Sini Heinonen<sup>3</sup>, Marcus Alvarez<sup>5</sup>, Kåre Inge  
6 Birkeland<sup>4</sup>, Christian André Drevon<sup>6</sup>, Päivi Pajukanta<sup>5,7,8</sup>, Adrian McCann<sup>9</sup>, Kirsi H. Pietiläinen<sup>3,10</sup>,  
7 Melina Claussnitzer<sup>11,12</sup>, Gunnar Mellgren<sup>1,2</sup>, Simon N. Dankel<sup>1,2†</sup>  
8

9 <sup>1</sup> Mohn Nutrition Research Laboratory, Department of Clinical Science, University of Bergen, Bergen,  
10 Norway

11 <sup>2</sup> Hormone Laboratory, Department of Medical Biochemistry and Pharmacology, Haukeland University  
12 Hospital, Bergen, Norway

13 <sup>3</sup> Obesity Research Unit, Research Program for Clinical and Molecular Metabolism, Faculty of  
14 Medicine, University of Helsinki, Finland

15 <sup>4</sup> The University of Oslo, Institute of Clinical Medicine, and Oslo University Hospital, Department of  
16 Transplantation Medicine, Oslo, Norway

17 <sup>5</sup> Department of Human Genetics, David Geffen School of Medicine at UCLA, Los Angeles, CA, USA

18 <sup>6</sup> The University of Oslo, Institute of Basic Medical Sciences, Department of Nutrition, Oslo, Norway

19 <sup>7</sup> Bioinformatics Interdepartmental Program, UCLA, Los Angeles, CA, USA

20 <sup>8</sup> Institute for Precision Health, David Geffen School of Medicine at UCLA, Los Angeles, CA, USA

21 <sup>9</sup> Bevitall A/S, Laboratoriebygget, Haukeland University Hospital, Bergen, Norway

22 <sup>10</sup> Obesity Center, Endocrinology, Abdominal Center, Helsinki University Hospital and University of  
23 Helsinki, Helsinki, Finland

24 <sup>11</sup> Broad Institute of MIT and Harvard, Cambridge, Massachusetts, USA

25 <sup>12</sup> Department of Medicine, Beth Israel Deaconess Medical Center, Harvard Medical School, Boston MA,  
26 USA  
27

28 \* These authors contributed equally.

29 † Corresponding author: Simon N. Dankel, PhD

30 Department of Clinical Science

31 University of Bergen

32 Haukeland University Hospital

33 N-5021 Bergen, Norway

34 ORCID: <https://orcid.org/0000-0001-6972-1824>

35 Phone: (+47 94 30 86 37)

36 e-mail: [simon.dankel@uib.no](mailto:simon.dankel@uib.no)  
37

38 **Keywords:** Adipocytes, Amino acid metabolism, Branched chain amino acids, Insulin resistance, Lipid  
39 storage, Obesity.

40 **Declaration of interests:** The authors declare no competing interests.

© The Author(s) 2023. Published by Oxford University Press on behalf of the Endocrine Society. This is an Open  
Access article distributed under the terms of the Creative Commons Attribution-NonCommercial-NoDerivs licence  
(<https://creativecommons.org/licenses/by-nc-nd/4.0/>), which permits non-commercial reproduction and distribution  
of the work, in any medium, provided the original work is not altered or transformed in any way, and that the work  
is properly cited. For commercial re-use, please contact [journals.permissions@oup.com](mailto:journals.permissions@oup.com)

## 1 **Abstract**

2 **Context:** The neutral amino acid transporter SLC7A10/ASC-1 is an adipocyte-expressed gene with  
3 reduced expression in insulin resistance and obesity. Inhibition of SLC7A10 in adipocytes was  
4 shown to increase lipid accumulation despite decreasing insulin-stimulated uptake of glucose, a  
5 key substrate for *de novo* lipogenesis. These data imply that alternative lipogenic substrates to  
6 glucose fuel continued lipid accumulation during insulin resistance in obesity.

7 **Objective:** We examined whether increased lipid accumulation during insulin resistance in  
8 adipocytes may involve alter flux of lipogenic amino acids dependent on SLC7A10 expression and  
9 activity, and whether this is reflected by extracellular and circulating concentrations of marker  
10 metabolites.

11 **Design:** In adipocyte cultures with impaired SLC7A10, we performed RNA-sequencing and  
12 relevant functional assays. By targeted metabolite analyses (GC-MS/MS), flux of all amino acids  
13 and selected metabolites were measured in human and mouse adipose cultures. Additionally,  
14 *SLC7A10* mRNA levels in human subcutaneous adipose tissue (SAT) were correlated to candidate  
15 metabolites and adiposity phenotypes in two independent cohorts.

16 **Results:** SLC7A10 impairment altered expression of genes related to metabolic processes  
17 including branched-chain amino acid (BCAA) catabolism, lipogenesis and glyceroneogenesis. In  
18 3T3-L1 adipocytes, SLC7A10 inhibition increased fatty acid uptake and cellular content of  
19 glycerol and cholesterol. SLC7A10 impairment in SAT cultures altered uptake of aspartate and  
20 glutamate, and increased the net uptake of BCAAs, while increasing the net release of the valine  
21 catabolite 3-hydroxyisobutyrate (3-HIB). In human cohorts, *SLC7A10* mRNA correlated inversely  
22 with total fat mass, circulating TAG, BCAAs and 3-HIB.

- 1 **Conclusion:** Reduced SLC7A10 activity strongly affects flux of BCAAs in adipocytes, which may
- 2 fuel continued lipogenesis during insulin resistance, and be reflected in increased circulating levels
- 3 of the valine-derived catabolite 3-HIB.

ACCEPTED MANUSCRIPT

## 1 **1. Introduction**

2 Altered adipose tissue function, in close association with systemic insulin resistance, adipocyte  
3 hypertrophy, local and systemic low-grade inflammation and ectopic lipid accumulation,  
4 contributes to chronic metabolic diseases such as type 2 diabetes and cardiovascular diseases (1–  
5 4). New insight into the cellular and molecular processes underlying lipid storage and insulin  
6 resistance may enable novel strategies for prevention and therapy. Mature white adipocytes store  
7 excess energy primarily as triacylglycerols (TAG) (5), and fatty acids (FAs) required for TAG  
8 synthesis are sourced from exogenous FA uptake (6) and *de novo* lipogenesis (7). While around  
9 60% of glycerol for TAG synthesis in the liver comes from pyruvate (8), TAG synthesis in  
10 adipocytes largely depends on glyceroneogenesis, a process functionally similar to hepatic  
11 gluconeogenesis (9,10). Activity of PC, PCK1 (PEPCK), and other glyceroneogenic enzymes  
12 expressed in adipocytes can drive glycerol formation from, e.g., lactate, pyruvate, and other TCA  
13 cycle intermediates, which partly also depends on the availability and metabolism of specific amino  
14 acids (11–14).

15  
16 Metabolomic analyses have revealed altered circulating concentrations of amino acids and  
17 metabolites related to insulin resistance (15), including the branched-chain amino acids (BCAAs;  
18 leucine, isoleucine, and valine). Genetic variants associated with insulin resistance modulate  
19 BCAA catabolic pathways, and activation of BCAA catabolism has been shown to improve insulin  
20 sensitivity and lipid metabolism in rats and mice (16). Moreover, variants associated with BCAA  
21 catabolic pathways are associated with an increased risk of type 2 diabetes (17,18). Elevated  
22 circulating BCAA levels partly depend on the loss of steps in BCAA catabolism and/or  
23 downregulation of enzymes responsible for BCAA oxidation in adipose tissue (15,19–22).

1 Increased catabolism of BCAAs during adipogenesis is associated with lipid accumulation (23,24)  
2 and suggests that these essential amino acids provide carbon for lipid and/or glycerol synthesis  
3 (25). Altered blood concentrations of BCAA-related metabolites have been found to reflect  
4 metabolic changes and mediate insulin resistance, and increased extracellular concentrations of 3-  
5 hydroxyisobutyrate (3-HIB) (26), a valine catabolite, is shown to be strongly associated with  
6 insulin resistance and type 2 diabetes (27). Higher 3-HIB levels reflect adipocyte lipid  
7 accumulation, and also directly influences core metabolic processes in white as well as brown  
8 adipocytes (27).

9  
10 Our recent studies revealed the sodium independent amino acid transporter SLC7A10 (also known  
11 as ASC-1), carrying small neutral amino acids such as serine, glycine and alanine, as a novel player  
12 regulating adipocyte lipid accumulation and metabolism in obesity and insulin resistance (28,29).  
13 *SLC7A10* mRNA expression in adipose tissue is highly heritable and correlates inversely with risk  
14 alleles in the *KLF14* type 2 diabetes risk locus, and is strongly associated with insulin resistance  
15 and adipocyte hypertrophy (30). In human primary and mouse 3T3-L1 adipose cultures, SLC7A10  
16 impairment reduced serine uptake, production of the antioxidant glutathione, mitochondrial  
17 respiration and insulin-stimulated glucose uptake, and increased reactive oxygen species  
18 generation and lipid accumulation (28). Another study, inhibiting the amino acid carrier in cultured  
19 human deep neck white adipocytes, confirmed reduction in serine uptake, but also found  
20 significantly reduced uptake of cysteine, glycine and alanine compared to controls (31). SLC7A10  
21 has recently also been implicated in thermogenesis and regulation of metabolism in different  
22 adipocyte subtypes (31–34). Therefore, understanding the effects of perturbed SLC7A10 activity  
23 in adipocytes in more detail may elucidate cellular and molecular pathways underlying the  
24 development of unhealthy adipose tissue expansion and insulin resistance. In particular, studying

1 the means by which SLC7A10 inhibition promotes lipid accumulation while suppressing insulin-  
2 stimulated glucose uptake can identify alternate carbon sources for lipogenesis in adipocytes.  
3 Additionally, identifying circulating biomarkers that reflect these cellular changes may allow  
4 earlier detection of adipose-dependent development of insulin resistance.

5  
6 In the present study, we examine changes in amino acid metabolism that may drive lipid  
7 accumulation in conditions of reduced insulin-stimulated glucose uptake, by profiling changes in  
8 the flux of amino acids and related metabolites in human adipocytes with and without  
9 pharmacologic inhibition of SLC7A10 activity. The clinical relevance of SLC7A10-dependent  
10 changes in the metabolism of BCAAs and other amino acids is supported by clinical cohorts  
11 showing strong correlations between adipose *SLC7A10* mRNA, circulating amino acid- and 3-HIB  
12 concentrations, adiposity traits, and systemic insulin resistance.

## 14 **2. Materials and methods**

### 15 **2.1 Ethics approval**

16 The study was approved by the relevant ethics committees (Regional Committee for Medical and  
17 Health Research Ethics (REC) West, Norway (Western Norway Obesity Biobank (WNOB), project  
18 2010/502); REC North, Norway (MyoGlu, project 2011/882); and the Ethics Committee of the  
19 Helsinki University Central Hospital, Finland (Dnro 270/13/03/01/2008). All study  
20 participants/sample donors gave written informed consent.

### 21 **2.2 Cell cultures**

#### 22 **2.2.1 Human primary adipose cultures and adipogenesis**

1 Human liposuction aspirates were collected with informed consent from the abdomen of donors  
2 operated at Plastikkirurg1 and Aleris medical center in Bergen, Norway. The donors were 10  
3 women and 1 man aged 21-68 years (mean±SD; 46.3±13.0) with BMI between 24-33 kg/m<sup>2</sup>  
4 (28.5±2.6) (**Supplementary Table 1**) (35). Following overnight incubation at 4 °C, subcutaneous  
5 liposuction aspirate was heated to 37 °C, the stromal vascular fraction (SVF) was isolated and the  
6 cultures were differentiated as previously described (28,36).

### 8 **2.2.2 Murine cell line cultures and adipogenesis**

9 Preparation, culturing and differentiation of mouse 3T3-L1 preadipocytes was performed using  
10 standard protocols described in detail previously (27).

### 12 **2.3 RNA sequencing**

13 RNA was isolated using RNeasy kit (QIAGEN) and cDNA-sequencing was performed using the  
14 Illumina HiSeq2000 platform. Reads were aligned using HiSat (Version 2.1.0), matrixed in  
15 featureCounts (Version 1.5.2) and analyzed using DESeq2 (Version 1.22.2) as described  
16 previously (28).

### 18 **2.4 Gene Set Enrichment Analysis (GSEA)**

19 47 gene sets for relevant metabolic processes were compiled from the publicly available databases  
20 KEGG (37), Reactome (38), Brenda (39), and HumanCyc (40) (**Supplementary Dataset 1**) (35).  
21 Using RNA sequencing data for vehicle (DMSO) and SLC7A10 inhibitor-treated human primary  
22 adipocytes, using the highly selective SLC7A10 inhibitor BMS-466442 (referred to as SLC7A10  
23 inhibitor) (41,42), we generated a ranked list of genes by multiplying -log<sub>10</sub> (adjusted P) value

1 with the sign of fold change (+ for  $\log_2FC > 0$  and - for  $\log_2FC < 0$ ) (28). Eight gene sets with less  
2 than 10 input genes were removed based on a minimum threshold of genes required per gene set.  
3 The remaining 39 gene sets were analyzed for enrichment using R package '*fgsea*' (version 1.14.0)  
4 and results were adjusted for multiple testing using false discovery rate (Benjamini-Hochberg  
5 method).

## 7 **2.5 Western blotting**

8 Cells were lysed in RIPA buffer (Thermo Fisher Scientific) supplemented with PhosStop™ (Sigma  
9 Aldrich), EDTA, sodium orthovanadate and protease inhibitor cocktail (Roche). The DC protein  
10 assay (Bio-Rad) was used to measure protein concentration in cell lysates, and equal amounts of  
11 sample lysate (15-30  $\mu\text{g}$ ) were loaded onto 4-20% TGX gels (Bio-Rad) and resolved by SDS-  
12 PAGE. Proteins were then transferred to a nitrocellulose membrane, which was blocked using 5%  
13 fatty acid-free milk or BSA. The following antibodies were used:  $\beta$ -actin (1:5000, Abcam, ab6276,  
14 AB\_2223210), HIBCH (1:200, Sigma Aldrich, HPA036541, AB\_2675182), and HRP goat anti-  
15 mouse IgG secondary antibody (1:7500, BD Biosciences, 554002, AB\_395198) and HRP goat anti-  
16 rabbit IgG secondary antibody (1:10000, Thermo Fischer Scientific, 31460, AB\_228341). Femto  
17 solution (Thermo Scientific) was used to produce luminescence, and densitometry was performed  
18 to calculate target protein amount relative to endogenous controls ( $\beta$ -actin).

## 20 **2.6 Metabolite analyses**

21 Medium from cell cultures was collected at 48-hour intervals, and amino acid and related  
22 metabolite levels in medium were measured by gas chromatography-tandem mass spectrometry  
23 (GC-MS/MS) based on methyl chloroformate derivatization at Bevitel AS (43). The method has  
24 been upgraded to include additional metabolites by adding ion-pairs for these analytes and

1 authentic isotope-labeled internal standards to the existing assay. The within- and between-day  
2 coefficient of variation for the assay ranged from 0.7-4.5% and 1.1-4.7%, respectively. The  
3 measured concentrations were used to calculate the influx and efflux of amino acids and  
4 metabolites relative to the unconditioned medium.

## 6 **2.7 Lipid staining**

7 Oil-red-O (ORO) staining was used to assess intracellular neutral lipid accumulation in cultured  
8 mature adipocytes (44). Intracellular ORO content was quantitated by measuring optical density  
9 absorbance at 500 nm using a spectrophotometer (SpectraMax PLUS384).

## 11 **2.8 Fatty acid uptake and intracellular content of glycerol and cholesterol**

12 Spectrophotometry-based kits were applied at 37°C according to the manufacturer's protocols. For  
13 FA uptake (MAK156; Sigma-Aldrich), 100  $\mu$ L/well of Fatty Acid Dye Loading Solution was  
14 added, and data were normalized to cell number/well using Hoechst staining. For glycerol (J3150,  
15 Promega) and cholesterol (J3190, Promega) content, data were normalized to DNA content per  
16 well.

## 18 **2.9 Hoechst staining**

19 Hoechst staining was performed by fixing cells in PBS containing 8% formaldehyde and Hoechst  
20 staining dye (1 $\mu$ g/mg) for a minimum of 1 hour. Subsequently, cell counts were obtained by  
21 counting of nuclei using a BD Pathway 855 (BD Bioscience) microscope and CellProfiler software.

## 23 **2.10 DNA quantification**

1 Double stranded DNA (dsDNA) content per well was measured using QuantiFluor® ONE dsDNA  
2 system (E4870, Promega) according to manufacturer's protocol.

3

## 4 **2.11 Human cohorts**

### 5 **2.11.1 The MyoGlu study**

6 The MyoGlu study was a controlled clinical exercise intervention trial (Clinical Trials Registration:  
7 NCT01803568) in sedentary (<1 exercise session/wk) in men aged 40 to 65 years of Scandinavian  
8 origin, performed in 2011-2012 in Oslo, Norway and is described in detail previously (45). The  
9 dysglycemic group (n = 11) had fasting glucose  $\geq 5.6$  mmol/L and/or 2-hour glucose  $\geq 7.8$  mmol/L  
10 and BMI 27–32 kg/m<sup>2</sup> (**Supplementary Table 2**) (35). Subjects with known hypertension, liver or  
11 kidney disease, chronic inflammatory disease, or on any medication expected to affect glucose  
12 metabolism (lipid lowering, anti-hypertensive, ASA, corticosteroids, etc.) were excluded. The  
13 control group (n = 13) of normoglycemic men of healthy weight had fasting glucose < 5.6 mmol/L  
14 and 2-hour OGTT < 7.8 mmol/L and without a family history of diabetes, and BMI 20.9–26.7  
15 kg/m<sup>2</sup> (**Supplementary Table 2**) (35). Insulin sensitivity was measured by hyperinsulinemic  
16 euglycemic clamp, and body composition and fatty liver were analyzed by magnetic resonance  
17 imaging and proton magnetic resonance spectroscopy MRI/MRS. Plasma amino acid  
18 concentrations were measured by liquid chromatography tandem mass spectrometry (LC-MS/MS),  
19 and plasma 3-hydroxyisobutyrate (3-HIB),  $\alpha$ -ketoglutarate and glycine concentrations by GC-  
20 MS/MS (43) at Bevital AS. mRNA from SAT was isolated and cDNA was deep sequenced using  
21 Illumina Hi-Seq 2000 (46). cDNA reads were aligned using Tophat v2.0.8. and quantified using  
22 HTSeq v0.6.1p.

23

### 24 **2.11.2 Twin cohorts**

1 A subset of 12 female and 7 male monozygotic twin pairs discordant for BMI (within-pair  
2 difference of BMI  $\geq 3$  kg/m<sup>2</sup>, n = 19 twin pairs; aged 22–36 years) were included from two  
3 population-based twin cohorts, FinnTwin16 (FT16) (47) and FinnTwin12 (FT12) (48)  
4 (**Supplementary Table 3**) (35). A BMI difference of BMI  $\geq 3$  kg/m<sup>2</sup> translates to a 10kg difference  
5 in body weight. In monozygotic twins, this was shown to exhibit significant within-twin pair  
6 differences in several clinical measures related to cardiometabolic health (49). Clinical data,  
7 adipose tissue transcriptomics and serum metabolite data were obtained as described previously  
8 (49,50). Briefly, body composition was assessed using dual-energy X-ray absorptiometry,  
9 abdominal subcutaneous and visceral adipose tissue volume was assessed by MRI, and liver fat  
10 percentage by MRS. Biochemical analytes were analyzed in fasting samples, including serum  
11 metabolites quantified by a high-throughput NMR metabolomics platform. In addition, Matsuda  
12 index was calculated from oral glucose tolerance tests (OGTT). mRNA from the SAT biopsies was  
13 isolated and cDNA was sequenced using the Illumina HiSeq2000 platform. cDNA reads were  
14 aligned using STAR v2.5.2b and quantified using HTSeq v0.6.1p.

15

## 16 **2.12 Statistics**

17 Results from cell culture experiments were assessed by a Box-Whiskers Tukey's test to identify  
18 and discard outliers. Two-tailed unpaired student's t-test was used to assess statistically significant  
19 differences between groups in cell culture assays. Correlations in the MyoGlu cohort were  
20 calculated by Spearman's rank correlation test. Differences between anthropometric and metabolic  
21 traits between twin pairs were assessed using matched- pairs signed-rank test for continuous  
22 variables. Regression analysis in twin individuals was performed using a linear model analysis (R  
23 package *lme4*). Metabolite levels and clinical traits were used as dependent variables, *SLC7A10*  
24 mRNA expression as an independent variable, and twinship as a random factor with adjustment for

1 age, sex and BMI. Regression models for delta values calculated between lean and heavy twins  
2 were not adjusted for BMI to preserve the study design. For all experiments statistical details and  
3 the number of biological samples (n) are provided in the figure legends. n annotates the number of  
4 parallel wells per treatment in cell experiments and the number of patients in clinical cohorts.  
5

ACCEPTED MANUSCRIPT

### 1 **3. Results**

#### 2 **SLC7A10 inhibition increases cellular levels of lipids and glycerol in adipocytes**

3 We previously showed that pharmacological inhibition of SLC7A10 activity promotes lipid  
4 accumulation while suppressing insulin-stimulated glucose uptake in cultured primary human and  
5 3T3-L1 mouse adipocytes, along with profound effects on global gene expression including key  
6 lipid markers, TCA cycle and glycolysis genes (28). We here investigated SLC7A10 inhibitor-  
7 induced effects on lipid metabolism more extensively. Short-term (24-hour) treatment of mature  
8 3T3-L1 adipocytes with SLC7A10 inhibitor reduced intracellular glycerol content compared to  
9 controls (**Figure 1A**), while there were no significant shorter-term differences in cellular fatty acid  
10 (FA) uptake or cholesterol content (**Figure 1A**). On the other hand, more persistent reduction in  
11 SLC7A10 activity during differentiation increased all these measures significantly (**Figure 1A**),  
12 suggesting a broad effect on lipid synthesis and storage.

13  
14 To uncover mechanisms contributing to the SLC7A10 inhibitor-mediated increase in fat storage in  
15 further detail, we examined effects of SLC7A10 inhibition on pathways of lipid and energy  
16 metabolism in human primary adipocyte cultures, using targeted GSEA with 47 manually curated  
17 comprehensive gene sets related to lipid and energy metabolism/substrate utilization. Consistent  
18 with the functional data, the transcriptome analysis showed significant enrichment of upregulated  
19 mRNAs in processes such as glycerophospholipid metabolism, TCA cycle, cholesterol  
20 biosynthesis, FA uptake, and TAG synthesis and catabolism (**Figure 1B-C**). Key transcription  
21 factors known to regulate many of these genes were also upregulated (**Figure 1C**).

#### 22 23 **Amino acids fuel adipocyte glyceroneogenesis and lipid biosynthesis**

1 The reduced insulin-stimulated glucose uptake previously observed following SLC7A10 inhibition  
2 in mature cultured human and mouse adipocytes (28) suggests that carbon sources other than  
3 glucose contributed to increased TAG formation and lipid accumulation (7). In human primary  
4 adipocyte cultures, short-term inhibition during mid-differentiation upregulated key genes  
5 involved in glyceroneogenesis (e.g., *PC* and *PCK1*) as well as glycerophospholipid metabolism  
6 (**Figure 2A, B**). FAs, cholesterol and glycerol can be synthesized *de novo* in fat cells using amino  
7 acids as precursors via the TCA cycle (51) (**Supplementary Figure 1**) (35). To assess whether  
8 amino acid catabolism provided precursors fueling lipogenesis when SLC7A10 activity was  
9 reduced, we analyzed gene sets related to the metabolism of all the major amino acids using GSEA.  
10 The analysis revealed a significant enrichment of up-regulated genes in the metabolism of BCAA,  
11 and to a lesser extent for metabolism of phenylalanine and tyrosine, aspartate and asparagine, and  
12 lysine (**Figure 3A**).

13 To obtain more direct evidence of altered amino acid consumption, we next performed targeted  
14 metabolite analysis of all amino acids throughout differentiation of primary human adipose cultures  
15 from 5 different donors, to determine whether the SLC7A10 inhibition-mediated transcript changes  
16 may have translated into altered amino acid consumption. In line with the RNA-sequencing data  
17 showing upregulated genes in BCAA metabolic pathways, the hourly uptake was increased for all  
18 three BCAAs when SLC7A10 activity was impaired (**Figure 3B**), particularly in mid-to-late  
19 differentiation (**Figure 3C**). Further analysis of the GSEA data from human primary adipocytes  
20 showed that the 20 leading edge genes in BCAA metabolism category included seven significantly  
21 upregulated genes, encoding the catabolic enzymes AACS, ACADM, ACADSB, ALDH6A1,  
22 BCKDHB, HIBADH, and HMGCS1 (**Figure 3D, E**). 3-hydroxyisobutyrate (3-HIB), a metabolite  
23 in the valine catabolic pathway implicated in adipocyte lipid accumulation and insulin resistance

1 (27), showed a substantial efflux upon SLC7A10 inhibition during differentiation (**Figure 3F**),  
2 with significant changes observed for days 8-12 in cultures from 5 different donors (**Figure G**). In  
3 line with the increase in 3-HIB efflux, protein expression of the rate-limiting 3-HIB-forming  
4 enzyme HIBCH, which removes the CoA from 3-HIB-CoA, was higher in differentiated human  
5 primary adipocytes after longer-term SLC7A10 inhibition compared to control (**Figure 3H**).

### 6 7 **SLC7A10 inhibition affects serine, alanine, aspartate, and glutamate flux and catabolism in** 8 **human adipocytes**

9 To examine whether amino acids other than the BCAAs may have contributed to fuel the observed  
10 increase in lipid accumulation in SLC7A10-impaired cells, not necessarily reflected in gene  
11 expression changes, we screened the medium collected throughout differentiation of cultured  
12 adipocytes from 5 different human donors for changes in the remaining 17 natural amino acids.  
13 We found no significant effects of SLC7A10 inhibition on any amino acids during the first four  
14 days of differentiation (**Supplementary Figure 2**) (35). This is in line with substantial increases  
15 in *SLC7A10* expression during later stages of adipocyte differentiation (28). Serine levels in the  
16 medium were, as shown previously (28), increased in response to SLC7A10 impairment most  
17 notably from days 8-12 of adipocyte differentiation, reflecting decreased uptake (**Figure 4A**,  
18 **Supplementary Figure 2**) (35). The small neutral amino acid alanine, earlier reported to be  
19 transported by SLC7A10 in the opposite direction to serine (29), showed reduced efflux from day  
20 8 to 16 of adipogenesis (**Figure 4A**, **Supplementary Figure 2**) (35).

21  
22 Interestingly, the cells switched from releasing more to taking up more aspartate throughout  
23 differentiation, and this switch was accentuated in the inhibitor-treated cells leading to more

1 pronounced aspartate uptake than observed for controls (**Supplementary Figure 2**) (35). The  
2 increased aspartate uptake was seen until day 12, followed by another switch to decreased uptake  
3 during days 12-16 (**Figure 4B, Supplementary Figure 2**) (35). Glutamate followed a similar  
4 pattern to that observed for aspartate, although without the initial decrease in uptake during day 4-  
5 6 (**Figure 4B, Supplementary Figure 2**) (35). These data indicate dynamic changes in the  
6 utilization of aspartate and glutamate in the metabolic situation of increased lipid accumulation and  
7 decreased insulin-stimulated glucose uptake upon SLC7A10 inhibition during adipogenesis. Both  
8 these non-essential amino acids are precursors of the TCA cycle intermediates oxaloacetate and  $\alpha$ -  
9 ketoglutarate, respectively (**Supplementary Figure 1**) (35), and may have contributed to fueling  
10 glyceroneogenesis and FA synthesis. Looking back into our GSEA analysis of the RNA-seq data,  
11 we found that 10 leading-edge genes drove enrichment of the serine metabolism (**Figure 3A**),  
12 where *ALAS1*, *AOC2*, *DMGDH* and *GRHPR* were significantly upregulated (**Figure 4C**). For  
13 aspartate and asparagine metabolism (**Figure 3A**), there were 6 leading-edge genes, including the  
14 significantly upregulated *ASPA*, *GOT1* and *NAT8L* (**Figure 4C, D**). Although no changes in the  
15 fluxes of phenylalanine and tyrosine were observed with SLC7A10 inhibition, enrichment of the  
16 metabolic pathway for these amino acids (**Figure 3A**) was driven by 5 leading-edge genes,  
17 including the significantly upregulated genes *QDPR*, *GOT1*, *FAH* and *AOC2* (**Figure 4C**).  
18 Moreover, the gene encoding GLS, the enzyme that converts glutamine to glutamate, was strongly  
19 downregulated in response to SLC7A10 inhibition (**Figure 4E**), and the medium concentration of  
20  $\alpha$ -ketoglutarate was markedly reduced in cultured adipocytes from 5 different donors (**Figure 4F**),  
21 suggesting increased consumption of this TCA metabolite. Taken together, these data indicate that  
22 impaired SLC7A10 function exerts potent effects on TCA cycle activity linked to amino acid  
23 uptake and metabolism, representing mechanisms that contribute to accelerated lipid accumulation.

24

1 ***SLC7A10* mRNA in SAT is reduced in dysglycemia and correlates inversely with body fat**  
2 **mass and plasma amino acid levels**

3 We next sought to corroborate the link between adipocyte *SLC7A10*, body fat distribution, and  
4 amino acid metabolism *in vivo*. We first compared *SLC7A10* mRNA in SAT from the MyoGlu  
5 study (46) between participants with normoglycemia (NG) and dysglycemia (DG) (n=26) (45).  
6 SAT *SLC7A10* mRNA expression was significantly lower in DG compared to NG participants  
7 (**Figure 5A**). We found medium to strong inverse correlations between SAT *SLC7A10* mRNA and  
8 BMI, total body fat mass and fat mass of most adipose depots, as well as circulating leptin and  
9 TAG levels and TAG/HDL ratio (a surrogate marker of insulin resistance) (**Figure 5B**).  
10 Interestingly, similar inverse correlations were observed between SAT *SLC7A10* mRNA and all  
11 the three BCAAs, 3-HIB, phenylalanine, and tyrosine, whereas insulin sensitivity (M-value  
12 assessed using euglycemic clamp) was positively associated with *SLC7A10* expression, although  
13 not significantly (**Figure 5B, C**).

14  
15 To validate these findings and assess the relative genetic and environmental contributions to the  
16 associations, we additionally investigated SAT *SLC7A10* expression in rare monozygotic twin  
17 pairs discordant for BMI (n=19) and found significantly lower *SLC7A10* mRNA expression in  
18 heavy compared to lean co-twins (**Figure 5D**). Consistent with the MyoGlu cohort, we found  
19 strong significant inverse associations in twin individuals between SAT *SLC7A10* expression and  
20 total, visceral, and hepatic fat, plasma glucose and insulin levels, HOMA-IR, CRP, circulating  
21 TAG, TAG/HDL, and total and LDL cholesterol. The Matsuda index, reflecting whole body insulin  
22 sensitivity, and HDL-C were positively associated with SAT *SLC7A10* expression (**Figure 5E**).  
23 When investigating the differences within each BMI-discordant twin-pair (delta values of heavy-  
24 lean co-twins), delta SAT *SLC7A10* mRNA correlated with deltas for visceral fat and clinical traits

1 related to insulin resistance such as HOMA-IR and TAG/HDL, suggesting a strong environmental  
2 regulation of these clinical phenotypes (**Supplementary Figure 3**) (35). Also consistent with the  
3 MyoGlu cohort, plasma levels of the BCAAs leucine and isoleucine, phenylalanine and tyrosine  
4 showed strong significant negative correlations with *SLC7A10* mRNA levels (**Figure 5E, F**).  
5 Overall, we observed an inverse association between *SLC7A10* expression and measures of body  
6 fat and clinical phenotype traits linked to insulin resistance, including plasma amino acid levels  
7 and the T2D-associated valine catabolite 3-HIB.

8

#### 9 **4. Discussion**

10 Our study provides new insights into substrate utilization and mechanisms underlying lipogenesis  
11 and fat storage in adipose tissue in conditions of impaired insulin-stimulated glucose uptake  
12 (considered a primary lipogenic substrate). We find that *SLC7A10* impairment alters adipocyte  
13 flux and metabolism of several amino acids, most notably BCAAs, but also serine, alanine,  
14 aspartate and glutamate. These changes are associated with effects on adipocyte FA uptake and  
15 intracellular glycerol and cholesterol levels. The physiological importance of *SLC7A10*-dependent  
16 alterations in adipocyte amino acid metabolism was supported by observations of strong inverse  
17 correlations between adipose *SLC7A10* mRNA expression and adiposity and cardiometabolic risk  
18 traits, as well as with circulating amino acid levels in human cohorts.

19 A primary finding is the augmented BCAA influx upon inhibition of *SLC7A10*, which is not  
20 characterized as a BCAA transporter, during mid-to-late stages of differentiation, along with  
21 upregulation of BCAA catabolic enzymes and increased lipid accumulation. Our observations in  
22 cultured human primary adipocytes expand on previous knowledge of increased uptake and  
23 catabolism of the BCAAs during adipocyte differentiation in mouse adipocytes, fueling lipogenesis

1 (23–25,27,52). Importantly, we provide novel data suggesting that the marked increase in BCAA  
2 catabolism contributed to increased fat storage during decreased insulin-stimulated glucose uptake  
3 in adipocytes. Differentiation of 3T3-L1 adipocytes was previously shown to involve a switch from  
4 consumption of glutamine and glucose to increased BCAA consumption in association with  
5 increased branched-chain fatty acid synthesis (24). Notably, during adipocyte differentiation,  
6 BCAA oxidation products appear to almost exclusively provide carbons for lipid synthesis as  
7 opposed to protein synthesis (52). Enhanced generation of amino acid catabolic intermediates (e.g.,  
8 propionyl-CoA and succinyl-CoA) can also shift their fate towards FA synthesis rather than beta-  
9 oxidation (53). Moreover, studies in 3T3-L1 adipocytes have shown that leucine and isoleucine  
10 accounts for 25% of the lipogenic acetyl-CoA, while valine and isoleucine contributes to 100% of  
11 propionyl-CoA that is used for lipogenesis (25). Of note, the BCAA catabolic enzyme BCKDH  
12 can generate high levels of mitochondrial reactive oxygen species (ROS) (54), linking our previous  
13 finding that SLC7A10 inhibition increases ROS generation (28) to an increase in BCAA  
14 breakdown. Given the possible causal role of increased ROS levels in lipid accumulation (55), such  
15 an effect of augmented BCAA catabolism on ROS might have also contributed to the higher lipid  
16 accumulation in adipocytes with impaired SLC7A10 function.

17  
18 Concomitant with the increased lipid accumulation and BCAA catabolism, we found a novel link  
19 between SLC7A10 expression/function, and adipocyte release and plasma levels of 3-HIB, a valine  
20 catabolite. Although the rate-limiting enzyme for 3-HIB formation, HIBCH, did not show a  
21 significant change in mRNA expression, its protein expression was highly increased by SLC7A10  
22 inhibition, uncovering a mechanism that could underlie the increased circulating 3-HIB observed  
23 in obesity and insulin resistance. The clinical importance of the valine degradation pathway and 3-  
24 HIB is supported by recent *in vivo* data linking high plasma 3-HIB levels to adiposity, prediabetes

1 and type 2 diabetes (27,56). 3-HIB has also been shown to have potential paracrine functions,  
2 increasing the uptake of FAs in endothelial cells from skeletal muscle (26) and in adipocytes (27).  
3 In line with our findings, a study of intestinal epithelial cells from piglets showed a 3-HIB-mediated  
4 upregulation of proteins involved in fatty acid transport and synthesis, accompanied by an increase  
5 in TAG synthesis and lipid droplet formation (57). Thus, increased 3-HIB production may have  
6 contributed to higher FA uptake and lipid storage with SLC7A10 inhibition.

7  
8 We also found that inhibition of SLC7A10 during adipocyte differentiation increased the total  
9 intracellular glycerol content. TAG synthesis in adipocytes largely depends on glyceroneogenesis  
10 (9,10) where glycerol is synthesized *de novo* using pyruvate formed from amino acids and lactate  
11 (11–13). Consistently, mRNA expression for PC and PCK1 (PEPCK), key enzymes determining  
12 the rate of glyceroneogenesis (58,59) were upregulated by SLC7A10 inhibition in primary human  
13 adipocytes. Different amino acids may have fueled glyceroneogenesis through pyruvate in our  
14 experiments. Although serine and alanine can be converted to pyruvate, reduced intracellular  
15 availability of these amino acids due to SLC7A10 inhibition suggests alternative substrates. In  
16 addition to reduced uptake of serine and alanine, Arianti and colleagues observed decreased uptake  
17 of cysteine, glycine and threonine in SLC7A10-inhibited human deep neck area-derived adipocytes  
18 (31). We did not observe changes in the flux of these amino acids during SLC7A10-impairment,  
19 which could be explained by our human primary adipocytes being derived from abdominal  
20 subcutaneous fat and not deep neck tissue. Our data also show that SLC7A10 impairment affected  
21 fluxes of aspartate, glutamate and  $\alpha$ -ketoglutarate, which can be utilized for biosynthesis of  
22 glycerol as well as lipids and glucose via the TCA cycle (60). Finally, although we observed no  
23 changes in tyrosine and phenylalanine flux in the *in vitro* differentiated human primary adipocytes,  
24 we found an enrichment of genes involved in the metabolism of these amino acids, as well as strong

1 correlations between their circulating levels and adipose *SLC7A10* mRNA in humans *in vivo*. Both  
2 tyrosine and phenylalanine are precursors for acetoacetyl-CoA (a substrate for cholesterol  
3 biosynthesis) and fumarate (a TCA-cycle intermediate). Along with BCAAs, circulating levels of  
4 phenylalanine and tyrosine show associations with HOMA-IR (61,62). A recent analysis from the  
5 METSIM study found elevated plasma levels of these aromatic amino acids to be associated with  
6 insulin resistance and low insulin secretion in type 2 diabetes, along with the other amino acids  
7 (BCAAs, aspartate, glutamate, and alanine) identified in our study (63).

8  
9 Furthermore, we observed increased mRNA expression of enzymes required for the synthesis of  
10 glycerophospholipids, which are essential for the formation of lipid droplets and their expansion  
11 (64). Additionally, we found that *SLC7A10* inhibition increased adipocyte cholesterol content.  
12 Cholesterol is essential for the maintenance of cell membrane structure and function as well as the  
13 formation of lipid droplets (65). Previous studies in rats show that *de novo* synthesis of cholesterol  
14 in adipocytes is as low as only 4% compared to that of liver (66). However, we observed a  
15 significant upregulation of enzymes involved in cholesterol biosynthesis in human adipocytes  
16 along with increased cholesterol content as measured in 3T3-L1 adipocytes after *SLC7A10*  
17 inhibition. Adipocyte cholesterol content, largely incorporated in cell membranes, correlates  
18 positively with fat cell size and is highly proportional to adipocyte triglyceride content (67), which  
19 is in line with our previously reported findings linking reduced adipose *SLC7A10* expression to  
20 increased adipocyte hypertrophy (28).

21  
22 The alterations in BCAA metabolism upon *SLC7A10* inhibition may be relevant for mechanisms  
23 affecting adipocyte beiging and thermogenesis, as BCAA metabolism has been implicated in  
24 brown adipocyte thermogenesis (32). Suwandi *et al.* showed that *Slc7a10* knockdown increased

1 the expression of brown/beige markers (68), while Arianti and coworkers proposed that Slc7a10  
2 may be important for brown adipocyte function (31). Although the present transcriptome analysis  
3 did not show any indications of altered adipocyte beiging upon SLC7A10 inhibition, further studies  
4 designed to explore the role of SLC7A10 perturbations in adipocyte beiging via altered amino acid  
5 metabolism should be performed.

6  
7 Notably, a link between BCAAs and SLC7A10 transporter activity was reported in neurons, where  
8 D-isoleucine was shown to enhance SLC7A10-mediated release of serine and glycine, in turn  
9 affecting the activity of the N-methyl D-aspartate (NMDA) glutamate receptor (69). Adipose  
10 tissues express genes involved in neurotransmitter signaling (70), including NMDA receptors as  
11 shown in multipotent stromal cells from human adipose tissue (71). A possible link to NMDA  
12 receptors in adipose tissue could also be relevant for the potent effect we observed of SLC7A10  
13 inhibition on glutamate transport.

14  
15 Ongoing discussions regarding the role of carbohydrates and insulin in the development of  
16 adipocytes and obesity (72) underscore the importance of better understanding lipid storage  
17 mechanisms. In this regard, our study contributes with new mechanistic insights by elucidating  
18 potential amino acid-related mechanisms involved in lipid accumulation in the context of reduced  
19 insulin-stimulated glucose uptake in adipocytes. However, the study has limitations. Suwandhi and  
20 coworkers found D-serine accumulation in mouse preadipocytes with perturbed Slc7a10 function  
21 (32), but we were in this study not able to assess effects on intracellular amino acid concentrations  
22 or to separate between the D- and L-stereoisomers of the amino acids. Studies with radiolabeled  
23 amino acids could provide more direct evidence for the conversion of specific amino acids into  
24 TCA cycle intermediates and their subsequent incorporation into lipids and lipid droplets in

1 adipocytes. The increased uptake of  $\alpha$ -ketoglutarate, an important cofactor for enzymes regulating  
2 chromatin modifications (51), could also be further explored in relation to the large effect of  
3 SLC7A10 inhibition on adipocyte gene expression. Additionally, more research is needed to reveal  
4 the mechanisms by which SLC7A10 inhibition increases BCAA uptake and catabolism, and to  
5 describe how this relates to evidence of decreases in specific steps of BCAA catabolism in adipose  
6 tissue of humans with insulin resistance (46,53,62).

#### 8 **4.1 Conclusion**

9 In conclusion, our data detailing SLC7A10-dependent gene expression and metabolite changes in  
10 human adipocytes and adipose tissue provide new insights into the mechanisms of continued lipid  
11 accumulation during insulin resistance. In particular, the increased uptake and catabolism of  
12 BCAAs during mid-to-late stages of adipocyte differentiation after SLC7A10 inhibition suggests  
13 that lipid accumulation during diminished insulin-stimulated glucose uptake involves diverting  
14 catabolism of BCAA and other amino acids towards FA and TAG synthesis, with efflux of 3-HIB  
15 as a potential measurable marker of these obesogenic processes.

#### 17 **Availability of data and materials**

18 The datasets generated and/or analyzed during the present study are available from the  
19 corresponding author upon reasonable request and the RNA-sequencing data are deposited in the  
20 National Center for Biotechnology Information (NCBI) Gene Expression Omnibus (GEO)  
21 (accession number GSE135156).

#### 23 **Author Contributions**

1 R.Å.J., D.S.P.T., L.S. and S.N.D. designed the study, carried out the experiments, analyzed and  
2 interpreted results, and wrote the manuscript. M.S.B assisted with experiments. S.L-Ø., K.I.B., and  
3 C.D. conducted the MyoGlu study, and S.L-Ø. analyzed the data. S.H. and K.H.P. contributed to  
4 sample/data collection in the twin cohorts, M.A., P.P. to generation and analysis of RNA-seq data,  
5 and M.M. and K.H.P. to the design, transcriptomics and metabolite data analysis, and interpretation  
6 for these cohorts. A.M. performed metabolite analyses. S.N.D. and G.M. facilitated the laboratory  
7 work. All authors reviewed and edited the manuscript. S.N.D. is the guarantor of this work and had  
8 full access to all the data in the study and takes responsibility for the integrity of the data and the  
9 accuracy of all the analyses.

10

## 11 **Funding**

12 We acknowledged the support from the Research Council of Norway (263124/F20), Western  
13 Norway Regional Health Authority, the Norwegian Diabetes Association, the Trond Mohn  
14 Foundation, and NovoNordisk Scandinavia AS. We also acknowledge the support from Academy  
15 of Finland, grant numbers 335443, 314383, 272376, 266286; Finnish Medical Foundation;  
16 Gyllenberg Foundation; Novo Nordisk Foundation, grant numbers NNF20OC0060547,  
17 NNF17OC0027232, NNF10OC1013354; Finnish Diabetes Research Foundation; University of  
18 Helsinki; Government Research Funds; and Helsinki University Hospital. The MyoGlu study was  
19 supported by grants from University of Oslo, Southeastern Regional Health Authorities, Anders  
20 Jahre's Foundation for Medical Research, EU-financed FP7 project (NutriTech grant agreement  
21 no: 289511), Freia Medical Research Foundation and The Johan Throne-Holst Foundation for  
22 Nutrition Research.

23

1 **Acknowledgements**

2 We thank the patients/study participants for providing samples and data, and all the organizations  
3 that funded our research. We thank Laurence Lawrence-Archer for support with gene expression  
4 analyses and Christian Busch at Plastikirurg1 for providing access to human liposuction aspirate.

5

ACCEPTED MANUSCRIPT

## 1 References

- 2 1. **Czech MP.** Mechanisms of insulin resistance related to white, beige, and brown  
3 adipocytes. *Mol. Metab.* 2020;34:27–42.
- 4 2. **Kim JI, Huh JY, Sohn JH, Choe SS, Lee YS, Lim CY, Jo A, Park SB, Han W, Kim  
5 JB.** Lipid-overloaded enlarged adipocytes provoke insulin resistance independent of  
6 inflammation. *Mol. Cell. Biol.* 2015;35(10):1686–99.
- 7 3. **Klötting N, Fasshauer M, Dietrich A, Kovacs P, Schön MR, Kern M, Stumvoll M,  
8 Blüher M.** Insulin-sensitive obesity. *Am. J. Physiol. - Endocrinol. Metab.* 2010;299(3).
- 9 4. **Acosta JR, Douagi I, Andersson DP, Bäckdahl J, Rydén M, Arner P, Laurencikiene  
10 J.** Increased fat cell size: a major phenotype of subcutaneous white adipose tissue in non-  
11 obese individuals with type 2 diabetes. *Diabetologia* 2016;59(3):560–570.
- 12 5. **Rodríguez A, Ezquerro S, Méndez-Giménez L, Becerril S, Frühbeck G.** Revisiting the  
13 adipocyte: A model for integration of cytokine signaling in the regulation of energy  
14 metabolism. *Am. J. Physiol. - Endocrinol. Metab.* 2015;309(8):E691–E714.
- 15 6. **Thompson BR, Lobo S, Bernlohr DA.** Fatty acid flux in adipocytes: The in's and out's  
16 of fat cell lipid trafficking. *Mol. Cell. Endocrinol.* 2010;318(1–2):24–33.
- 17 7. **Collins JM, Neville MJ, Pinnick KE, Hodson L, Ruyter B, Van Dijk TH, Reijngoud  
18 DJ, Fielding MD, Frayn KN.** De novo lipogenesis in the differentiating human adipocyte  
19 can provide all fatty acids necessary for maturation. *J. Lipid Res.* 2011;52(9):1683–1692.
- 20 8. **Kalhan SC, Mahajan S, Burkett E, Reshef L, Hanson RW.** Glyceroneogenesis and the  
21 Source of Glycerol for Hepatic Triacylglycerol Synthesis in Humans. *J. Biol. Chem.*  
22 2001;276(16):12928–12931.
- 23 9. **Nye C, Kim J, Kalhan SC, Hanson RW.** Reassessing triglyceride synthesis in adipose  
24 tissue. *Trends Endocrinol. Metab.* 2008;19(10):356–361.
- 25 10. **Nye CK, Hanson RW, Kalhan SC.** Glyceroneogenesis is the dominant pathway for  
26 triglyceride glycerol synthesis in vivo in the rat. *J. Biol. Chem.* 2008;283(41):27565–  
27 27574.
- 28 11. **Phosphoenolpyruvate Carboxykinase and the Synthesis of Glyceride-Glycerol from  
29 Pyruvate in Adipose Tissue.** Available at:  
30 <https://www.jbc.org/content/242/11/2746.short>. Accessed April 6, 2020.
- 31 12. **Reshef L, Niv J, Shapiro B.** Effect of propionate on pyruvate metabolism in adipose  
32 tissue. *J. Lipid Res.* 1967;8(6):688–691.
- 33 13. **Reshef L, Hanson \$ R W, Ballard FJ.** *Glyceride-glycerol synthesis from pyruvate.*  
34 *Adaptive changes in phosphoenolpyruvate carboxykinase and pyruvate carboxylase in*  
35 *adipose tissue and liver.*; 1969. Available at: <https://www.jbc.org/content/244/8/1994.long>.
- 36 14. **Reshef L, Olswang Y, Cassuto H, Blum B, Croniger CM, Kalhan SC, Tilghman SM,  
37 Hanson RW.** Glyceroneogenesis and the triglyceride/fatty acid cycle. *J. Biol. Chem.*  
38 2003;278(33):30413–30416.

- 1 15. **Newgard CB, An J, Bain JR, Muehlbauer MJ, Stevens RD, Lien LF, Haqq AM, Shah**  
2 **SH, Arlotto M, Slentz CA, Rochon J, Gallup D, Ilkayeva O, Wenner BR, Yancy WS,**  
3 **Eisenson H, Musante G, Surwit RS, Millington DS, Butler MD, Svetkey LP.** A  
4 branched-chain amino acid-related metabolic signature that differentiates obese and lean  
5 humans and contributes to insulin resistance. *Cell Metab.* 2009;9(4):311–26.
- 6 16. **White PJ, McGarrah RW, Grimsrud PA, Tso S-C, Yang W-H, Haldeman JM,**  
7 **Grenier-Larouche T, An J, Lapworth AL, Astapova I, Hannou SA, George T, Arlotto**  
8 **M, Olson LB, Lai M, Zhang G-F, Ilkayeva O, Herman MA, Wynn RM, Chuang DT,**  
9 **Newgard CB.** The BCKDH Kinase and Phosphatase Integrate BCAA and Lipid  
10 Metabolism via Regulation of ATP-Citrate Lyase. *Cell Metab.* 2018;27(6):1281-1293.e7.
- 11 17. **Lotta LA, Scott RA, Sharp SJ, Burgess S, Luan J, Tillin T, Schmidt AF, Imamura F,**  
12 **Stewart ID, Perry JRB, Marney L, Koulman A, Karoly ED, Forouhi NG, Sjögren**  
13 **RJO, Näslund E, Zierath JR, Krook A, Savage DB, Griffin JL, Chaturvedi N,**  
14 **Hingorani AD, Khaw K-T, Barroso I, McCarthy MI, O’Rahilly S, Wareham NJ,**  
15 **Langenberg C.** Genetic Predisposition to an Impaired Metabolism of the Branched-Chain  
16 Amino Acids and Risk of Type 2 Diabetes: A Mendelian Randomisation Analysis. *PLoS*  
17 *Med.* 2016;13(11). doi:10.1371/JOURNAL.PMED.1002179.
- 18 18. **Mahendran Y, Jonsson A, Have CT, Allin KH, Witte DR, Jørgensen ME, Grarup N,**  
19 **Pedersen O, Kilpeläinen TO, Hansen T.** Genetic evidence of a causal effect of insulin  
20 resistance on branched-chain amino acid levels. *Diabetol.* 2017 605 2017;60(5):873–878.
- 21 19. **Lackey DE, Lynch CJ, Olson KC, Mostaedi R, Ali M, Smith WH, Karpe F,**  
22 **Humphreys S, Bedinger DH, Dunn TN, Thomas AP, Oort PJ, Kieffer DA, Amin R,**  
23 **Bettaieb A, Haj FG, Permana P, Anthony TG, Adams SH.** Regulation of adipose  
24 branched-chain amino acid catabolism enzyme expression and cross-adipose amino acid  
25 flux in human obesity. *Am. J. Physiol. Metab.* 2013;304(11):E1175–E1187.
- 26 20. **Neinast MD, Jang C, Hui S, Murashige DS, Chu Q, Morscher RJ, Li X, Zhan L,**  
27 **White E, Anthony TG, Rabinowitz JD, Arany Z.** Quantitative Analysis of the Whole-  
28 Body Metabolic Fate of Branched-Chain Amino Acids. *Cell Metab.* 2019;29(2):417-  
29 429.e4.
- 30 21. **She P, Van Horn C, Reid T, Hutson SM, Cooney RN, Lynch CJ.** Obesity-related  
31 elevations in plasma leucine are associated with alterations in enzymes involved in  
32 branched-chain amino acid metabolism. *Am. J. Physiol. Metab.* 2007;293(6):E1552–  
33 E1563.
- 34 22. **Herman MA, She P, Peroni OD, Lynch CJ, Kahn BB.** Adipose tissue branched chain  
35 amino acid (BCAA) metabolism modulates circulating BCAA levels. *J. Biol. Chem.*  
36 2010;285(15):11348–56.
- 37 23. **Halama A, Horsch M, Kastenmüller G, Möller G, Kumar P, Prehn C, Laumen H,**  
38 **Hauner H, Hrabě de Angelis M, Beckers J.** Metabolic switch during adipogenesis: From  
39 branched chain amino acid catabolism to lipid synthesis. *Arch. Biochem. Biophys.*  
40 2016;589:93–107.
- 41 24. **Green CR, Wallace M, Divakaruni AS, Phillips SA, Murphy AN, Ciaraldi TP,**

- 1 **Metallo CM.** Branched-chain amino acid catabolism fuels adipocyte differentiation and  
2 lipogenesis. *Nat Chem Biol* 2016;12(1):15–21.
- 3 25. **Crown SB, Marze N, Antoniewicz MR.** Catabolism of Branched Chain Amino Acids  
4 Contributes Significantly to Synthesis of Odd-Chain and Even-Chain Fatty Acids in 3T3-  
5 L1 Adipocytes. Tochtrop GP, ed. *PLoS One* 2015;10(12):e0145850.
- 6 26. **Jang C, Oh SF, Wada S, Rowe GC, Liu L, Chan MC, Rhee J, Hoshino A, Kim B,  
7 Ibrahim A, Baca LG, Kim E, Ghosh CC, Parikh SM, Jiang A, Chu Q, Forman DE,  
8 Lecker SH, Krishnaiah S, Rabinowitz JD, Weljie AM, Baur JA, Kasper DL, Arany  
9 Z.** A branched-chain amino acid metabolite drives vascular fatty acid transport and causes  
10 insulin resistance. *Nat. Med.* 2016;22(4):421–426.
- 11 27. **Nilsen MS, Jersin RÅ, Ulvik A, Madsen A, McCann A, Svensson P-A, Svensson ME,  
12 Nedrebø BG, Gudbrandsen OA, Tell GS, Kahn CR, Ueland PM, Mellgren G, Dankel  
13 SN.** 3-Hydroxyisobutyrate, a Strong Marker of Insulin Resistance in Type 2 Diabetes and  
14 Obesity That Modulates White and Brown Adipocyte Metabolism. *Diabetes*  
15 2020;db191174.
- 16 28. **Jersin R, Tallapragada DSP, Madsen A, Skartveit L, Fjære E, McCann A, Dyer L,  
17 Willems A, Bjune JI, Bjune MS, Våge V, Nielsen HJ, Thorsen HL, Nedrebø BG,  
18 Busch C, Steen VM, Blüher M, Jacobson P, Svensson PA, Fernø J, Rydén M, Arner  
19 P, Nygård O, Claussnitzer M, Ellingsen S, Madsen L, Sagen J V., Mellgren G, Dankel  
20 SN.** Role of the Neutral Amino Acid Transporter SLC7A10 in Adipocyte Lipid Storage,  
21 Obesity, and Insulin Resistance. *Diabetes* 2021;70(3):680–695.
- 22 29. **Fukasawa Y, Segawa H, Kim JY, Chairoungdua A, Kim DK, Matsuo H, Cha SH,  
23 Endou H, Kanai Y.** Identification and characterization of a Na(+)-independent neutral  
24 amino acid transporter that associates with the 4F2 heavy chain and exhibits substrate  
25 selectivity for small neutral D- and L-amino acids. *J. Biol. Chem.* 2000;275(13):9690–8.
- 26 30. **Small KS, Todorčević M, Civelek M, Moustafa JSE-S, Wang X, Simon MM,  
27 Fernandez-Tajes J, Mahajan A, Horikoshi M, Hugill A, Glastonbury CA, Quaye L,  
28 Neville MJ, Sethi S, Yon M, Pan C, Che N, Viñuela A, Tsai P-C, Nag A, Buil A,  
29 Thorleifsson G, Raghavan A, Ding Q, Morris AP, Bell JT, Thorsteinsdottir U,  
30 Stefansson K, Laakso M, Dahlman I, Arner P, Gloyn AL, Musunuru K, Lusi AJ,  
31 Cox RD, Karpe F, McCarthy MI.** Regulatory variants at KLF14 influence type 2  
32 diabetes risk via a female-specific effect on adipocyte size and body composition. *Nat.*  
33 *Genet.* 2018 504 2018;50(4):572.
- 34 31. **Arianti R, Vinnai BÁ, Tóth BB, Shaw A, Csósz É, Vámos A, Gyóry F, Fischer-  
35 Posovszky P, Wabitsch M, Kristóf E, Fésüs L.** ASC-1 transporter-dependent amino acid  
36 uptake is required for the efficient thermogenic response of human adipocytes to  
37 adrenergic stimulation. *FEBS Lett.* 2021;595(16):2085–2098.
- 38 32. **Suwandhi L, Altun I, Karlina R, Miok V, Wiedemann T, Fischer D, Walzthoeni T,  
39 Lindner C, Böttcher A, Heinzmann SS, Israel A, Khalil AEMM, Braun A, Pramme-  
40 Steinwachs I, Burtscher I, Schmitt-Kopplin P, Heinig M, Elsner M, Lickert H, Theis  
41 FJ, Ussar S.** Asc-1 regulates white versus beige adipocyte fate in a subcutaneous stromal  
42 cell population. *Nat. Commun.* 2021;12(1):1–12.

- 1 33. **Jersin RÅ, Jonassen LR, Dankel SN.** The neutral amino acid transporter SLC7A10 in  
2 adipose tissue, obesity and insulin resistance. *Front. Cell Dev. Biol.* 2022;10:1889.
- 3 34. **Brøer S.** Amino acid transporters as modulators of glucose homeostasis. *Trends*  
4 *Endocrinol. Metab.* 2022;33(2):120–135.
- 5 35. **Jersin RÅ, Tallapragada DSP, Skartveit L, Bjune MS, Muniandy M, Lee-Ødegård S,**  
6 **Heinonen S, Alvarez M, Birkeland KI, Drevon CA, Pajukanta P, McCann A,**  
7 **Pietiläinen KH, Claussnitzer M, Mellgren G, Dankel SN.** Supplementary material and  
8 dataset from: Impaired adipocyte SLC7A10 promotes lipid storage in association with  
9 insulin resistance and altered BCAA metabolism. *DataverseNO* 2023.  
10 doi:<https://doi.org/10.18710/IMMHH2>.
- 11 36. **Lee MJ, Fried SK.** *Optimal protocol for the differentiation and metabolic analysis of*  
12 *human adipose stromal cells.* 1st ed. Elsevier Inc.; 2014. doi:10.1016/B978-0-12-800280-  
13 3.00004-9.
- 14 37. **Kanehisa M, Goto S.** KEGG: Kyoto Encyclopedia of Genes and Genomes. *Nucleic Acids*  
15 *Res.* 2000;28(1):27–30.
- 16 38. **Jassal B, Matthews L, Viteri G, Gong C, Lorente P, Fabregat A, Sidiropoulos K,**  
17 **Cook J, Gillespie M, Haw R, Loney F, May B, Milacic M, Rothfels K, Sevilla C,**  
18 **Shamovsky V, Shorser S, Varusai T, Weiser J, Wu G, Stein L, Hermjakob H,**  
19 **D'Eustachio P.** The reactome pathway knowledgebase. *Nucleic Acids Res.*  
20 2020;48(D1):D498–D503.
- 21 39. **Schomburg I, Chang A, Schomburg D.** BRENDA, enzyme data and metabolic  
22 information. *Nucleic Acids Res.* 2002;30(1):47–49.
- 23 40. **Romero P, Wagg J, Green ML, Kaiser D, Krummenacker M, Karp PD.**  
24 Computational prediction of human metabolic pathways from the complete human  
25 genome. *Genome Biol.* 2005;6(1). doi:10.1186/gb-2004-6-1-r2.
- 26 41. **Brown JM, Hunihan L, Prack MM, Harden DG, Bronson J, Dzierba CD, Gentles**  
27 **RG, Hendricson A, Krause R, Macor JE, Westphal RS.** In vitro Characterization of a  
28 small molecule inhibitor of the alanine serine cysteine transporter -1 (SLC7A10). *J.*  
29 *Neurochem.* 2014;129(2):275–83.
- 30 42. **Mikou A, Cabayé A, Goupil A, Bertrand HO, Mothet JP, Acher FC.** Asc-1  
31 Transporter (SLC7A10): Homology Models And Molecular Dynamics Insights Into The  
32 First Steps Of The Transport Mechanism. *Sci. Rep.* 2020;10(1):1–12.
- 33 43. **Midttun Ø, McCann A, Aarseth O, Krokeide M, Kvalheim G, Meyer K, Ueland PM.**  
34 Combined Measurement of 6 Fat-Soluble Vitamins and 26 Water-Soluble Functional  
35 Vitamin Markers and Amino Acids in 50 µL of Serum or Plasma by High-Throughput  
36 Mass Spectrometry. *Anal. Chem.* 2016;88(21):10427–10436.
- 37 44. **Bjune J-I, Dyer L, Røsland G V., Tronstad KJ, Njølstad PR, Sagen J V., Dankel SN,**  
38 **Mellgren G.** The homeobox factor Irx3 maintains adipogenic identity. *Metabolism*  
39 2019:154014.
- 40 45. **Langleite TM, Jensen J, Norheim F, Gulseth HL, Tangen DS, Kolnes KJ, Heck A,**

- 1 **Storås T, Grøthe G, Dahl MA, Kielland A, Holen T, Noreng HJ, Stadheim HK,**  
2 **Bjørnerud A, Johansen EI, Nellesmann B, Birkeland KI, Drevon CA.** Insulin  
3 sensitivity, body composition and adipose depots following 12 w combined endurance and  
4 strength training in dysglycemic and normoglycemic sedentary men. *Arch. Physiol.*  
5 *Biochem.* 2016;122(4):167–179.
- 6 46. **Lee S, Gulseth HL, Langleite TM, Norheim F, Olsen T, Refsum H, Jensen J,**  
7 **Birkeland KI, Drevon CA.** Branched-chain amino acid metabolism, insulin sensitivity  
8 and liver fat response to exercise training in sedentary dysglycaemic and normoglycaemic  
9 men. *Diabetologia* 2021;64(2):410–423.
- 10 47. **Kaidesoja M, Aaltonen S, Bogl LH, Heikkilä K, Kaartinen S, Kujala UM,**  
11 **Kärkkäinen U, Masip G, Mustelin L, Palviainen T, Pietiläinen KH, Rottensteiner M,**  
12 **Sipilä PN, Rose RJ, Keski-Rahkonen A, Kaprio J.** FinnTwin16: A Longitudinal Study  
13 from Age 16 of a Population-Based Finnish Twin Cohort. *Twin Res. Hum. Genet.*  
14 2019;22(6):530–539.
- 15 48. **Rose RJ, Salvatore JE, Aaltonen S, Barr PB, Bogl LH, Byers HA, Heikkilä K,**  
16 **Korhonen T, Latvala A, Palviainen T, Ranjit A, Whipp AM, Pulkkinen L, Dick DM,**  
17 **Kaprio J.** FinnTwin12 Cohort: An Updated Review. *Twin Res. Hum. Genet.*  
18 2019;22(5):302–311.
- 19 49. **van der Kolk BW, Saari S, Lovric A, Arif M, Alvarez M, Ko A, Miao Z,**  
20 **Sahebekhtari N, Muniandy M, Heinonen S, Oghabian A, Jokinen R, Jukarainen S,**  
21 **Hakkarainen A, Lundbom J, Kuula J, Groop P-H, Tukiainen T, Lundbom N,**  
22 **Rissanen A, Kaprio J, Williams EG, Zamboni N, Mardinoglu A, Pajukanta P,**  
23 **Pietiläinen KH.** Molecular pathways behind acquired obesity: adipose tissue and skeletal  
24 muscle multiomics in monozygotic twin pairs discordant for BMI. *Cell Reports Med.*  
25 2021:100226.
- 26 50. **Rämö JT, Kaye SM, Jukarainen S, Bogl LH, Hakkarainen A, Lundbom J, Lundbom**  
27 **N, Rissanen A, Kaprio J, Matikainen N, Pietiläinen KH.** Liver fat and insulin  
28 sensitivity define metabolite profiles during a glucose tolerance test in young adult twins.  
29 *J. Clin. Endocrinol. Metab.* 2017;102(1):220–231.
- 30 51. **Felix JB, Cox AR, Hartig SM.** Acetyl-CoA and Metabolite Fluxes Regulate White  
31 Adipose Tissue Expansion. *Trends Endocrinol. Metab.* 2021;32(5):320–332.
- 32 52. **Estrada-Alcalde I, Tenorio-Guzman MR, Tovar AR, Salinas-Rubio D, Torre-**  
33 **Villalvazo I, Torres N, Noriega LG.** Metabolic Fate of Branched-Chain Amino Acids  
34 During Adipogenesis, in Adipocytes From Obese Mice and C2C12 Myotubes. *J. Cell.*  
35 *Biochem.* 2017;118(4):808–818.
- 36 53. **Newgard CB.** Interplay between lipids and branched-chain amino acids in development of  
37 insulin resistance. *Cell Metab.* 2012;15(5):606–614.
- 38 54. **Ribas V, García-Ruiz C, Fernández-Checa JC.** Glutathione and mitochondria. *Front.*  
39 *Pharmacol.* 2014;5:151.
- 40 55. **Jones IV AR, Meshulam T, Oliveira MF, Burritt N, Corkey BE.** Extracellular Redox  
41 Regulation of Intracellular Reactive Oxygen Generation, Mitochondrial Function and

- 1 Lipid Turnover in Cultured Human Adipocytes. López Lluch G, ed. *PLoS One*  
2 2016;11(10):e0164011.
- 3 56. **Dankel SN.** 3-Hydroxyisobutyrate (3-HIB): Features and Links as a Biological Marker in  
4 Diabetes. 2022:1–12.
- 5 57. **Xu M, Che L, Niu L, Wang L, Li M, Jiang D, Deng H, Chen W, Jiang Z.** Molecular  
6 mechanism of valine and its metabolite in improving triglyceride synthesis of porcine  
7 intestinal epithelial cells. *Sci. Reports 2023 131* 2023;13(1):1–10.
- 8 58. **Millward CA, DeSantis D, Hsieh CW, Heaney JD, Pisano S, Olswang Y, Reshef L,**  
9 **Beidelschies M, Puchowicz M, Croniger CM.** Phosphoenolpyruvate carboxykinase  
10 (Pck1) helps regulate the triglyceride/fatty acid cycle and development of insulin  
11 resistance in mice. *J. Lipid Res.* 2010;51(6):1452–1463.
- 12 59. **Kumashiro N, Beddow SA, Vatner DF, Majumdar SK, Cantley JL, Guebre-**  
13 **Egzabher F, Fat I, Guigni B, Jurczak MJ, Birkenfeld AL, Kahn M, Perler BK,**  
14 **Puchowicz MA, Manchem VP, Bhanot S, Still CD, Gerhard GS, Petersen KF, Cline**  
15 **GW, Shulman GI, Samuel VT.** Targeting pyruvate carboxylase reduces gluconeogenesis  
16 and adiposity and improves insulin resistance. *Diabetes* 2013;62(7):2183–2194.
- 17 60. **Martínez-Reyes I, Chandel NS.** Mitochondrial TCA cycle metabolites control physiology  
18 and disease. *Nat. Commun.* 2020;11(1). doi:10.1038/s41467-019-13668-3.
- 19 61. **Wurtz P, Soininen P, Kangas AJ, Rönnemaa T, Lehtimäki T, Kähönen M, Viikari JS,**  
20 **Raitakari OT, Ala-Korpela M.** Branched-chain and aromatic amino acids are predictors  
21 of insulin resistance in young adults. *Diabetes Care* 2013;36(3):648–655.
- 22 62. **Wiklund P, Zhang X, Pekkala S, Autio R, Kong L, Yang Y, Keinänen-Kiukaanniemi**  
23 **S, Alen M, Cheng S, DeFronzo RA, Tripathy D, Muoio DM, Newgard CB, Abbasi F,**  
24 **Brown BW, Lamendola C, McLaughlin T, Reaven GM, Lee J, Hollenbeck C, Reaven**  
25 **GM, Karelis AD, St-Pierre DH, Conus F, Rabasa-Lhoret R, Poehlman ET,**  
26 **Ferrannini E, Boden G, Lynch CJ, Adams SH, Wang TJ, Wiklund PK, Guilherme A,**  
27 **Virbasius J V., Puri V, Czech MP, Kahn SE, Hull RL, Utzschneider KM, Kabir SM,**  
28 **Lee ES, Son DS, Soronen J, Hardy OT, Boden G, Shulman GI, Shulman GI, Arner P,**  
29 **Ryden MF, Karpe F, Dickmann JR, Frayn KN, Felig P, Marliss E, Cahill GF,**  
30 **McCormack SE, Newgard CB, Sunny NE, Krebs M, Tremblay F, Gougeon R, Bolea**  
31 **S, Pertusa JA, Martin F, Sanchez-Andres J V., Soria B, Yang J, She P, Leskinen T,**  
32 **Masoodi M, Kuda O, Rossmeisl M, Flachs P, Kopecky J, Kern PA, Gregorio GB Di,**  
33 **Lu T, Rassouli N, Ranganathan G, Zimmet PZ, Segal KR, Landt M, Klein S, Tilg H,**  
34 **Moschen AR, Pietilainen KH, Weisberg SP, Cinti S, Cline GW, Krssak M, Patti ME,**  
35 **Rome S, Meugnier E, Wang Q, Cheng S, Borra RJ, Soininen P, Matsuda M,**  
36 **DeFronzo RA, Bolstad BM, Irizarry RA, Astrand M, Speed TP, Gentleman RC,**  
37 **Gautier L, Cope L, Bolstad BM, Irizarry R, Y HYB.** Insulin resistance is associated  
38 with altered amino acid metabolism and adipose tissue dysfunction in normoglycemic  
39 women. *Sci. Rep.* 2016;6:24540.
- 40 63. **Vangipurapu J, Stancáková A, Smith U, Kuusisto J, Laakso M.** Nine amino acids are  
41 associated with decreased insulin secretion and elevated glucose levels in a 7.4-year  
42 follow-up study of 5,181 Finnish men. *Diabetes* 2019;68(6):1353–1358.

- 1 64. **Olzmann JA, Carvalho P.** Dynamics and functions of lipid droplets. *Nat. Rev. Mol. Cell*  
2 *Biol.* 2019;20(3):137–155.
- 3 65. **Fujimoto T, Parton RG.** Not just fat: The structure and function of the lipid droplet. *Cold*  
4 *Spring Harb. Perspect. Biol.* 2011;3(3):1–17.
- 5 66. **Angel A, Bray GA.** Synthesis of fatty acids and cholesterol by liver, adipose tissue and  
6 intestinal mucosa from obese and control patients. *Eur. J. Clin. Invest.* 1979;9(5):355–362.
- 7 67. **Le Lay S, Ferré P, Dugail I.** Adipocyte cholesterol balance in obesity. In: *Biochemical*  
8 *Society Transactions*. Vol 32. Biochem Soc Trans; 2004:103–106.
- 9 68. **Yoneshiro T, Wang Q, Tajima K, Matsushita M, Maki H, Igarashi K, Dai Z, White**  
10 **PJ, McGarrah RW, Ilkayeva OR, Deleye Y, Oguri Y, Kuroda M, Ikeda K, Li H,**  
11 **Ueno A, Ohishi M, Ishikawa T, Kim K, Chen Y, Sponton CH, Pradhan RN, Majd H,**  
12 **Greiner VJ, Yoneshiro M, Brown Z, Chondronikola M, Takahashi H, Goto T,**  
13 **Kawada T, Sidossis L, Szoka FC, McManus MT, Saito M, Soga T, Kajimura S.**  
14 **BCAA catabolism in brown fat controls energy homeostasis through SLC25A44.** *Nature*  
15 2019;572(7771):614–619.
- 16 69. **Rosenberg D, Artoul S, Segal AC, Kolodney G, Radzishevsky I, Dikopoltsev E, Foltyn**  
17 **VN, Inoue R, Mori H, Billard J-M, Wolosker H.** Neuronal d-Serine and Glycine  
18 Release Via the Asc-1 Transporter Regulates NMDA Receptor-Dependent Synaptic  
19 Activity. *J. Neurosci.* 2013;33(8).
- 20 70. **Nicolaysen A, Gammelsaeter R, Storm-Mathisen J, Gundersen V, Iversen PO.** The  
21 components required for amino acid neurotransmitter signaling are present in adipose  
22 tissues. *J. Lipid Res.* 2007;48(10):2123–2132.
- 23 71. **Kulikov A V., Rzhabinova AA, Goldshtein D V., Boldyrev AA.** Expression of NMDA  
24 receptors in multipotent stromal cells of human adipose tissue under conditions of retinoic  
25 acid-induced differentiation. *Bull. Exp. Biol. Med.* 2007;144(4):626–629.
- 26 72. **Speakman JR, Hall KD.** Carbohydrates, insulin, and obesity. *Science*  
27 2021;372(6542):577–578.

28

## 1 **Figure legends**

### 2 **Figure 1. SLC7A10 inhibition increases cellular levels of lipids and glycerol in adipocytes.**

3 Mouse 3T3-L1 preadipocytes and human primary adipose cultures were induced to differentiate  
4 for 8 days, and effects of pharmacological SLC7A10 inhibition on specific metabolic pathways  
5 were examined by functional assays (A) and gene expression analysis (RNA-sequencing) (B-C).  
6 Global gene expression from human adipose cultures treated with DMSO or SLC7A10 inhibitor  
7 (BMS-10 $\mu$ M) for 24 hours (days 7-8) was measured by RNA-sequencing (n = 6 pairs of DMSO  
8 vs. inhibitor from donors 1-6) (B-C).

9 **A.** 3T3-L1 preadipocytes were treated with DMSO (control) or SLC7A10 inhibitor (BMS-10 $\mu$ M)  
10 for short (days 7-8)- and long-term (days 2-8) during adipogenic differentiation. Effect of  
11 SLC7A10 inhibition on fatty acid uptake (n = 18-20) and the intracellular content of glycerol (n =  
12 16-20) and cholesterol (n = 16-18) are measured as described in the methods. Data are presented  
13 as median  $\pm$  IQR.

14 **B.** Gene set enrichment analysis (GSEA) based on gene sets of relevant metabolic pathways  
15 sourced mainly from Reactome and KEGG. The distribution of up- and downregulated genes are  
16 shown within the entire RNA-sequencing dataset ranked by signed fold change multiplied by –  
17  $\log_{10}$ (-P value) (the top-scoring up- and downregulated genes at the outer left and outer right,  
18 respectively). Pathways with significant enrichment of top-scoring genes for up- and  
19 downregulated genes combined are shown here.

20 **C.** mRNA expression of the GSEA leading edge genes in selected processes (including classical  
21 adipogenic markers/transcription factors) are shown, with indication of significance levels from  
22 the RNA-sequencing analysis adjusted for multiple testing. Data are presented as median  $\pm$  IQR.  
23 FA, fatty acid; FDR, false discovery rate; NES, normalized enrichment score; TF, transcription  
24 factor.

25 \*, p < 0.05; \*\*, p < 0.01; \*\*\*, p < 0.001.

26  
27 **Figure 2. SLC7A10 inhibition upregulates genes involved in glyceroneogenesis and**  
28 **glycerophospholipid metabolism.** Human primary adipose cultures were induced to  
29 differentiate for 8 days and treated with DMSO (control) or SLC7A10 inhibitor (BMS-10 $\mu$ M) for  
30 24 hours (days 7-8). Effects on specific metabolic pathways were examined using RNA-  
31 sequencing (n = 6 pairs of DMSO vs. SLC7A10 inhibitor from donors 1-6).

32 **A.** mRNA expression of the GSEA leading edge genes for glycerol(gluco)neogenesis and  
33 glycerophospholipid metabolism with indication of significance levels from the RNA-sequencing  
34 analysis adjusted for multiple testing. Data are presented as median  $\pm$  IQR.

35 **B.** Schematic overview of glycerol(gluco)neogenesis and glycerophospholipid metabolism. Red  
36 color indicated upregulated genes and blue color indicates downregulated genes.

37 \*, p < 0.05; \*\*, p < 0.01; \*\*\*, p < 0.001.

38  
39 **Figure 3. SLC7A10 inhibition in adipocytes increases BCAA consumption and release of 3-**  
40 **hydroxyisobutyrate.** Human primary adipose cultures were induced to differentiate and effects  
41 of pharmacological SLC7A10 inhibition on amino acid (AA) metabolic pathways and fluxes  
42 were examined by gene expression analysis, GC-MS/MS and western blotting.

- 1 **A.** Global gene expression was measured by RNA-sequencing after treating the adipose cultures  
2 with either DMSO (control) or SLC7A10 inhibitor (BMS-10 $\mu$ M) for 24 hours (days 7-8) (n = 6  
3 pairs of DMSO vs. SLC7A10 inhibitor from donors 1-6). Gene set enrichment analysis (GSEA)  
4 based on genes in AA pathways obtained mainly from Reactome and KEGG. The distribution of  
5 up- and downregulated genes is shown within the entire RNA-sequencing dataset ranked by  
6 signed fold change multiplied by  $-\log_{10}(-P \text{ value})$  (the top-scoring up- and downregulated genes  
7 at the outer left and outer right, respectively).
- 8 **B.** Average net hourly flux of BCAA for 48 hours was calculated by subtracting the  
9 concentrations in conditioned from concentrations in matched unconditioned medium, divided by  
10 48 (n = 2 for a representative experiment, donor 9).
- 11 **C.** Medium concentrations measured in duplicate were calculated for each 48-hour period  
12 normalized to the DMSO control. Data are presented as mean  $\pm$  SD (n = 5 individuals for days 6-  
13 8 and 10-12, donors 7-11 and n = 3 individuals for days 8-10, donors 9-11).
- 14 **D.** mRNA expression of the GSEA leading edge genes in the BCAA pathways are shown, with  
15 indication of significance levels from the RNA-sequencing analysis adjusted for multiple testing.  
16 Data are presented as median  $\pm$  IQR.p
- 17 **E.** Simplified schematic overview of the BCAA catabolic pathway. Red color indicated  
18 upregulated genes and blue color indicates downregulated genes by SLC7A10 inhibitor found by  
19 RNA-sequencing.
- 20 **F.** Average net hourly flux of 3-HIB for 48 hours was calculated by subtracting the  
21 concentrations in conditioned from concentrations in matched unconditioned medium, divided by  
22 48 (n=2 for a representative experiment, donor 9).
- 23 **G.** Medium concentrations measured in duplicate were calculated for each 48-hour period  
24 normalized to DMSO (control) and relative values per period are shown. Data are presented as  
25 mean  $\pm$  SD (n = 5 individuals for days 6-8 and 10-12, donors 7-11 and n = 3 individuals for days  
26 8-10, donors 9-11).
- 27 **H.** Protein levels of HIBCH (top) and the quantitative values of HIBCH relative to  $\beta$ -actin in  
28 human primary adipose culture treated with DMSO (control) or SLC7A10 inhibitor (BMS-  
29 10 $\mu$ M) from days 3-12 during adipogenic differentiation and assayed on day 12. Data are  
30 represented as individual points (n = 2 from a representative experiment, donor 11).  
31 BCAA, branched-chain amino acids.  
32 \*, p < 0.05; \*\*, p < 0.01; \*\*\*, p < 0.001.  
33

34 **Figure 4. SLC7A10 inhibition alters aspartate, glutamate, and  $\alpha$ -ketoglutarate flux during**  
35 **differentiation of human primary adipocytes.** Human primary adipose cultures were induced  
36 to differentiate and effects of pharmacological SLC7A10 inhibition on amino acid (AA) fluxes  
37 were examined by collecting culture medium every 48 hours, and its amino acid concentrations  
38 measured by GC-MS/MS.

- 39 **A, B, F.** Medium concentrations measured in duplicate were calculated for each 48-hour period  
40 normalized DMSO (control) and relative values per period are shown. Data are presented as  
41 mean  $\pm$  SD (n = 5 individuals for days 6-8 and 10-12, donors 7-11 and n = 3 individuals for days  
42 8-10, donors 9-11).
- 43 **C, E.** mRNA expression of the GSEA leading edge genes in the indicated pathways are shown,  
44 with indication of significance levels from the RNA-sequencing analysis adjusted for multiple  
45 testing. Data are presented as median  $\pm$  IQR.

1 **D.** Simplified schematic overview of amino acid metabolism related to the TCA cycle  
2 components oxaloacetate and  $\alpha$ -ketoglutarate. Red color indicates upregulated genes and blue  
3 color indicates downregulated genes.

4 \*,  $p < 0.05$ ; \*\*,  $p < 0.01$ ; \*\*\*,  $p < 0.001$ .

6 **Figure 5. *SLC7A10* mRNA expression in subcutaneous adipose tissue correlates with**  
7 **adiposity, insulin-resistance related metabolic traits and circulating amino acid metabolites**  
8 ***in vivo*.** Subcutaneous adipose tissue (SAT) was collected from people with or without  
9 dysglycemia in the MyoGlu study (baseline values,  $n = 26$ ) and from BMI-discordant  
10 monozygotic twin pairs ( $n = 19$  pairs).

11 **A.** MyoGlu participants were divided into two groups: normoglycemia (NG) and dysglycemia  
12 (DG) based on the glucose infusion rate measured during hyperinsulinemic euglycemic clamp  
13 ( $n=26$ ). *SLC7A10* expression was measured in SAT by mRNA sequencing and compared  
14 between both the groups. Data (RPKM normalized counts) are presented as median  $\pm$  IQR.

15 **B-C.** SAT *SLC7A10* mRNA expression was correlated to adiposity traits, insulin-resistance  
16 related metabolic traits, as well as, amino acids, and amino acid metabolites. Data are presented  
17 as Spearman ( $\rho$ ) correlation coefficients (unadjusted), outlined circles indicate statistically  
18 significant correlations ( $p < 0.05$ ).

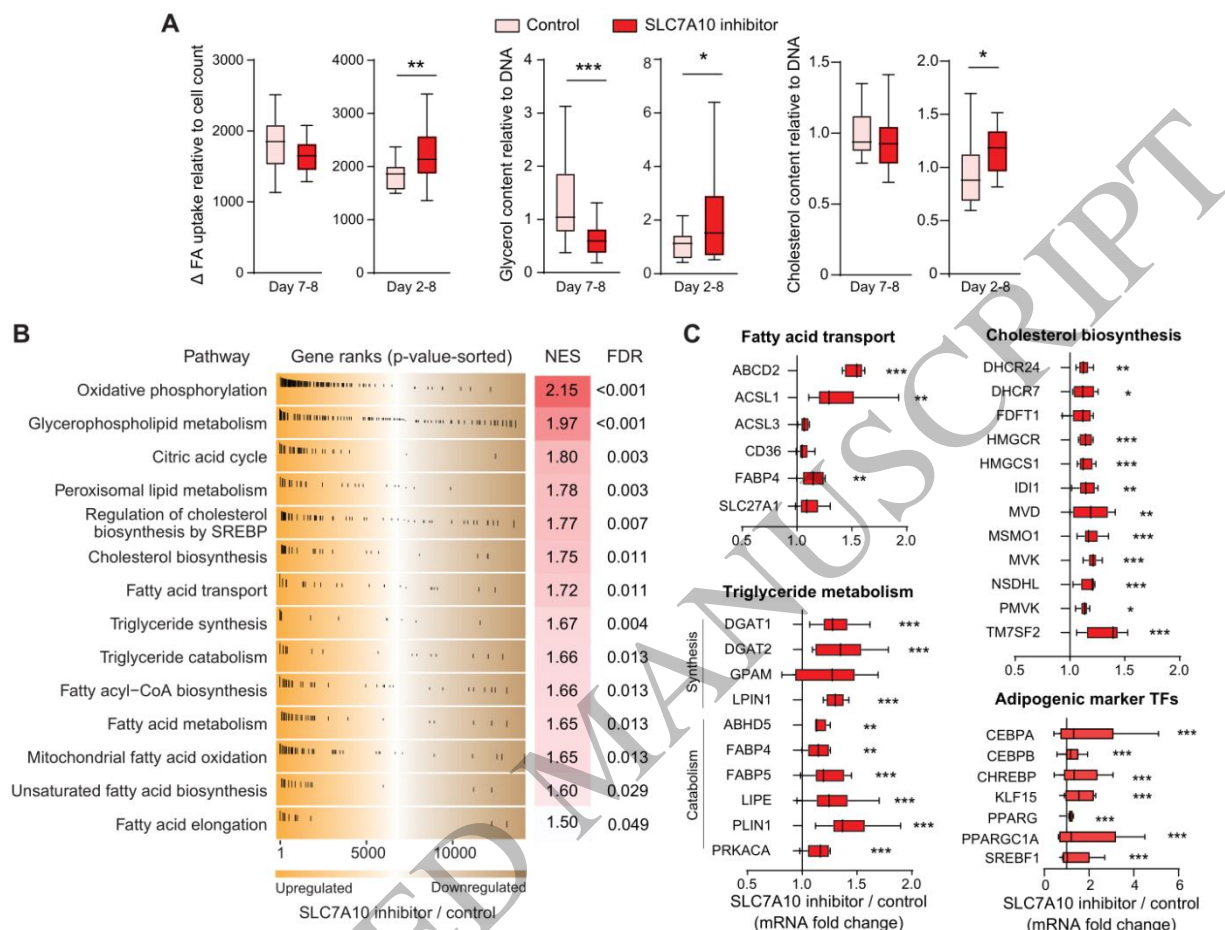
19 **D.** SAT *SLC7A10* expression was measured of BMI-discordant monozygotic twin pairs by  
20 mRNA-sequencing. Data (trimmed mean of M value (TMM) normalized counts) are presented  
21 with matched lines within twin pairs ( $n = 19$ ).

22 **E.** Association in twin individuals between SAT *SLC7A10* mRNA expression and adiposity  
23 traits, insulin-resistance related metabolic traits and select amino acids was assessed using linear-  
24 mixed models adjusted for age, sex, twinship and BMI. Data are plotted as standardized beta  
25 regression coefficients with standard error ( $\beta \pm SE$ ), outlined circles indicate statistically  
26 significant correlations.

27 **F.** Circulating amino acid levels of leucine, isoleucine, phenylalanine, and tyrosine measured in  
28 BMI-discordant monozygotic twin pairs by nuclear magnetic resonance (NMR) metabolomics  
29 are presented here with matched lines within twin pairs ( $n = 19$ ).

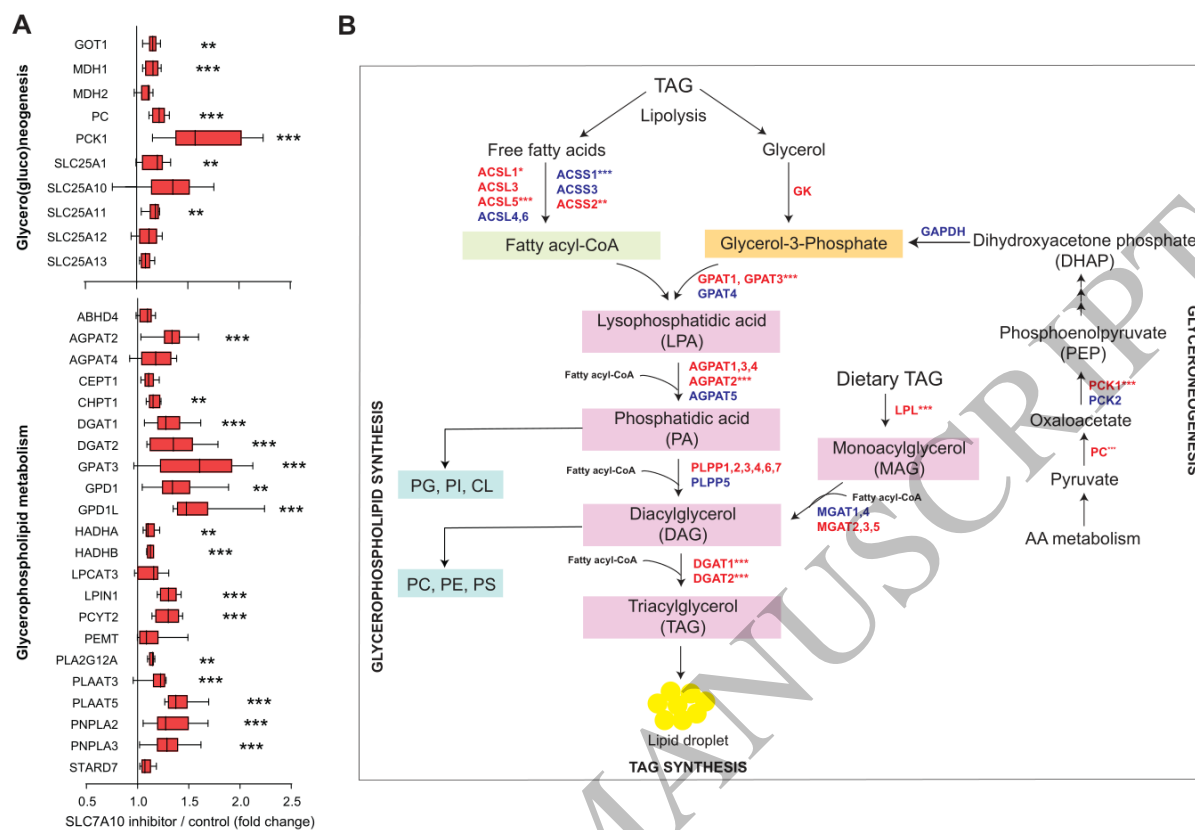
30 \*,  $p < 0.05$ ; \*\*\*,  $p < 0.001$ .

1 **Figures**



2

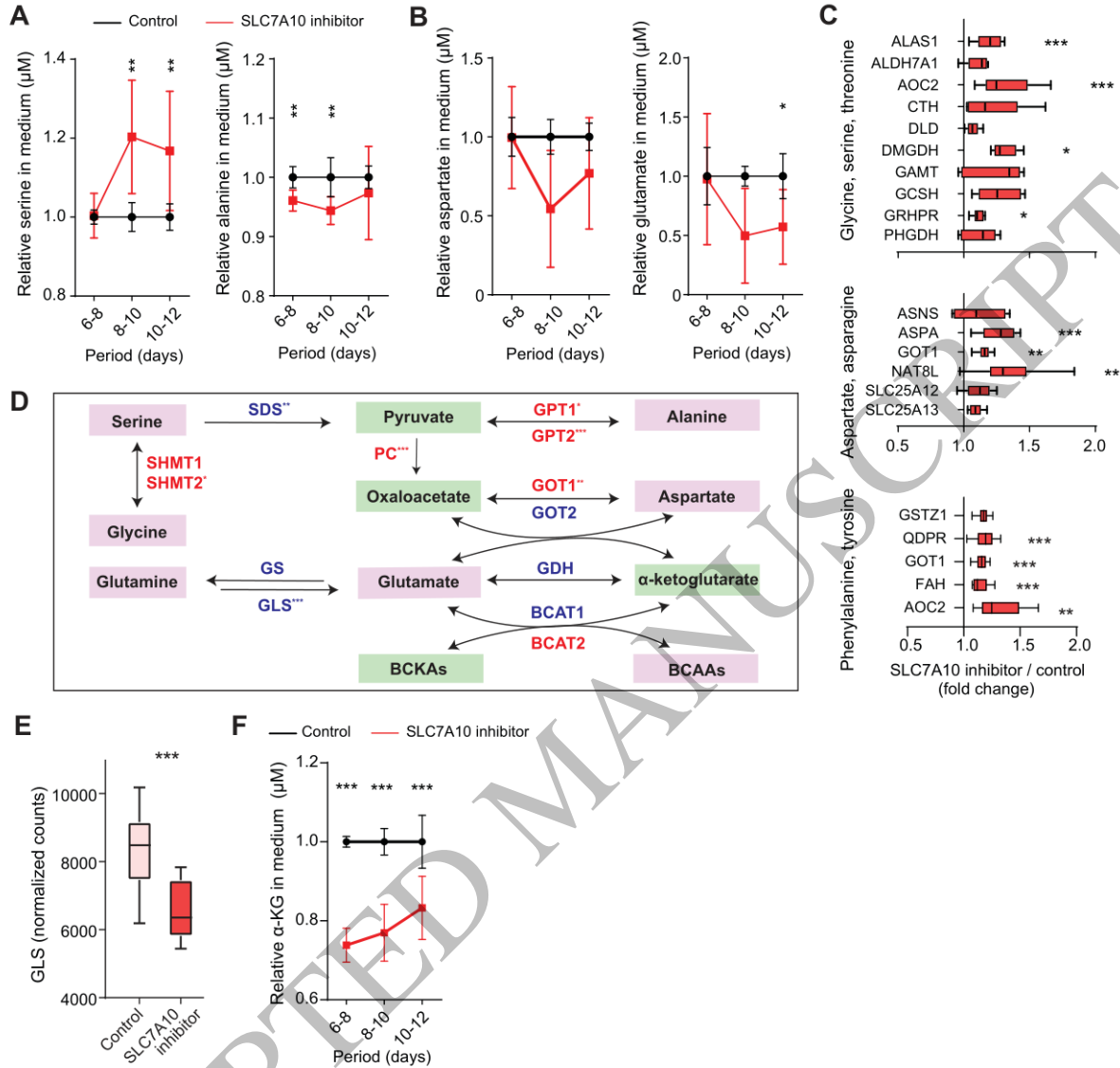
3 **Figure 1.**



1  
2

**Figure 2.**





1  
2 **Figure 4.**

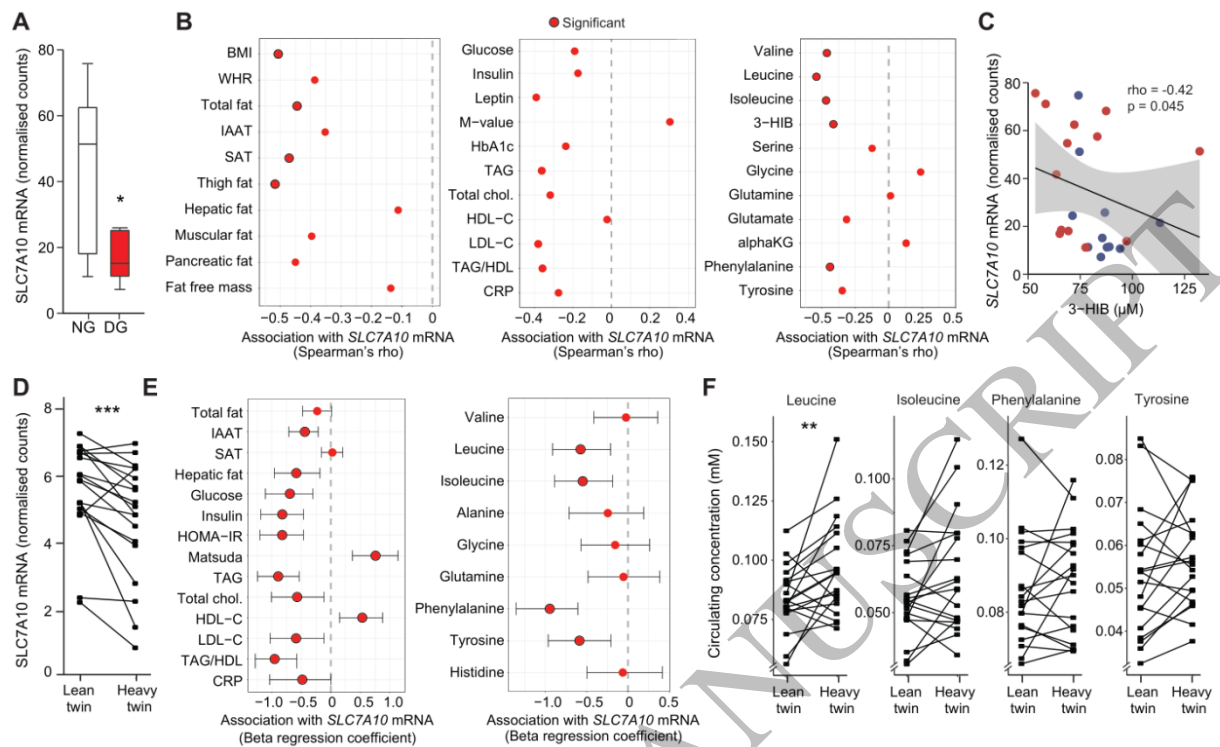


**Figure 5.**

1  
2  
3